CLINICAL REPORT

AMERICAN JOURNAL OF medical genetics PART A

Identification of a Novel de Novo Deletion in *RAF1* Associated With Biventricular Hypertrophy in Noonan Syndrome

Maria Elena Sana,[1] Andrea Spitaleri,[2] Dimitrios Spiliotopoulos,[2] Laura Pezzoli,[1] Laura Preda,[3] Giovanna Musco,[2] Paolo Ferrazzi,[4] and Maria Iascone[1]*

[1]USSD Laboratorio di Genetica Medica, Azienda Ospedaliera Papa Giovanni XXIII, Bergamo, Italy

[2]Biomolecular NMR Laboratory, Dulbecco Telethon Institute c/o Center of Translational Genomics and Bioinformatics, Fondazione Centro San Raffaele, Milan, Italy

[3]Centro per la Diagnosi e il Trattamento delle Cardiopatie Congenite, Dipartimento Cardiovascolare, Azienda Ospedaliera Papa Giovanni XXIII, Bergamo, Italy

[4]Surgical Centre for Cardiomyopathies and Valvular Diseases, Policlinico di Monza, Monza, Italy

Manuscript Received: 3 December 2013; Manuscript Accepted: 1 April 2014

Biventricular hypertrophy (BVH) is a disease state characterized by the thickening of the ventricle walls. The differential diagnosis of BVH with other congenital and familial diseases in which increased ventricle wall thickness is a prominent clinical feature is fundamental due to its therapeutic and prognostic value, mainly during infancy. We describe a 2-month-old infant presenting BVH. Using exome sequencing, we identified a novel de novo 3-bp deletion in the *RAF1* gene that is located in the binding active site for the 14-3-3 peptide. Based on docking calculations, we demonstrate that this novel mutation impairs protein/target binding, thus constitutively activating Ras signaling, which is a dysregulation associated with Noonan syndrome. Finally, our study underlines the importance of molecular modeling to understand the roles of novel mutations in pathogenesis.

Key words: biventricular hypertrophy; *RAF1*; exome sequencing; computational modeling; 14-3-3 protein; Noonan syndrome

How to Cite this Article:
Sana ME, Spitaleri A, Spiliotopoulos D, Pezzoli L, Preda L, Musco G, Ferrazzi P, Iascone M. 2014. Identification of a novel de novo deletion in *RAF1* associated with biventricular hypertrophy in Noonan syndrome.
Am J Med Genet Part A 164A:2069–2073.

INTRODUCTION

Biventricular hypertrophy (BVH) is defined as a disease state characterized by thickening of the left and right ventricle walls in a non-dilated ventricular chamber [Jain et al., 1999]. BVH can occur as a phenotype in a number of inherited syndromes with defects that produce systemic as well as cardiac manifestations. In this heterogeneous group, RASopathies are developmental syndromes caused by germline mutations in genes that encode components or regulators of the Ras/mitogen-activated protein kinase (MAPK) pathway [Tidyman and Rauen, 2009]. The diagnoses of various RASopathies, such as Noonan syndrome (OMIM #163950), LEOPARD syndrome (Noonan syndrome-multiple lentigines) (OMIM #151100) and related disorders [Schubbert et al., 2007], present an important challenge during the first months of life, as different etiologies may have different treatments and prognoses [Rauen, 2013]. Moreover, these syndromes are characterized by phenotypic heterogeneity and overlapping clinical manifestations that make differential diagnosis difficult.

We report on a 2-month-old male who was originally diagnosed with biventricular hypertrophy, mild dysmorphic features and without a family history of cardiovascular diseases. Exome sequencing revealed a novel de novo heterozygous in-frame 3-bp deletion in the *RAF1* gene, which encodes the serine-threonine kinase RAF1, one of the direct downstream effectors of Ras. Germline mutations in the *RAF1* gene account for approximately 3–5% of cases of

Grant sponsor: Fondazione S.Martino-CREBERG; Grant sponsor: Fondazione Cariplo.

*Correspondence to:
Maria Iascone, Genetica Molecolare, USSD Lab. Genetica Medica, Azienda Ospedaliera Papa Giovanni XXIII, Piazza OMS, 1 24127 Bergamo, Italy.
E-mail: miascone@hpg23.it

Article first published online in Wiley Online Library (wileyonlinelibrary.com): 29 April 2014
DOI 10.1002/ajmg.a.36588

Noonan syndrome [Wu et al., 2011]. In particular, sixteen different causative *RAF1* mutations, all missense, have been reported [Kobayashi et al., 2010]. Furthermore, hypertrophic cardiomyopathy occurs as a clinical feature in 95% of patients with mutations in the *RAF1* gene [Pandit et al., 2007; Razzaque et al., 2007]. Interestingly, this deletion falls in the C-terminal region of the RAF1 protein. Functional studies revealed that the amino-terminal region of the RAF1 protein interacts with 14-3-3 adaptor-scaffold proteins that are essential for the maintenance of Raf-1 phosphorylation and kinase activity [Fantl et al., 1994; Thorson et al., 1998; Kobayashi et al., 2010]. Molzan et al. [2010] demonstrated that C-terminal RAF1 mutations impaired binding to 14-3-3 proteins in patients with Noonan syndrome. To assess the role of this mutation in the structure and function of the protein, computational modeling calculations were performed.

CLINICAL REPORT

The patient was the first child of healthy, nonconsanguineous Italian parents, whose family history was unremarkable with respect to cardiovascular diseases. Polyhydramnios had been present during pregnancy. He was born at 37 weeks and weighed 3,080 g, with a one minute Apgar score of 9. He was breastfed, grew normally and exhibited constant weight gain. At 1 month, diagnostic assessment revealed systolic heart murmur, and echocardiography showed biventricular hypertrophy, mainly on the left side (left wall thickness 18 mm; right wall thickness 14 mm; interventricular septum 11 mm). He was hemodynamically stable under beta-blocker therapy. The left ventricular outflow tract (LVOT) pressure gradient was 22 mmHg as measured by continuous-wave Doppler echocardiography; the ejection fraction was 90%, and fractional shortening was 30%. Moreover, the patient had mildly dysmorphic features consisting of low-set posteriorly rotated ears, ocular hypertelorism, and prognathism. No café-au-lait spots or lentigines were observed. Bilateral cryptorchidism was also present. Neurobehavioral assessment was normal for his age. Since clinical features overlap and differential diagnosis was critical, exome sequencing was performed.

MATERIALS AND METHODS

After written informed consent, exome sequencing was performed on genomic DNA isolated using standard techniques from the patient and parents blood. Using this method, exons from all isoforms of 2,761 known disease-causing genes were assessed using the Illumina TruSight Exome enrichment kit and sequenced using a 2×150-bp paired-end protocol on an Illumina MiSeq following the manufacturer's instructions (Illumina, San Diego, CA). The raw data were analyzed using a standard pipeline based on the current best practices [DePristo et al., 2011], as previously reported [Sana et al., 2011; Iascone et al., 2012]. The threshold for mapping quality and base quality was set to a minimum Phred score = 20 [Ewing and Green, 1998; Ewing et al., 1998], which implies that, on average, 1 in 100 bases is not correct. Variants identified by sequencing were classified based on their potential effect on protein translation (splicing, missense, nonsense, and frameshift). The Human Gene Mutation Database (HGMD) Professional (Release 2013.2) [Stenson et al., 2009] was used to connect mutations and variants in genes to specific phenotypes. Using the dbSNP Release 137 [Sherry et al., 2001] Exome Sequencing Project (NHLBI-ESP) (ESP6500 data release) [http://snp.gs.washington.edu/EVS/] and 1000 Genomes Project (1KGP) databases [The 1000 Genomes Project Consortium, 2012], variants with minor allele frequency (MAF) >1% were filtered out. Using "abnormal facial shape" (HP:0001999) and "hypertrophic cardiomyopathy" (HP:0001639) as keywords, Human Phenotype Ontology (HPO) [Robinson et al., 2008] was used to prioritize gene variants. Finally, de novo and recessive inheritance models were applied in a filtering strategy. All detected variants were assessed using visual inspection with the Integrative Genomics Viewer (IGV) [Robinson et al., 2011] and were independently validated using Sanger sequencing. Molecular docking calculations of the wild-type and modified RAF1 peptide, RST-SEP-TPNVH and RST-SEP-TPIH, respectively (SEP is the phosphorylated serine residue), onto the 14-3-3ζ protein were performed using the HADDOCK-2.1 software [de Vries et al., 2007]. The modified RAF1 peptide was built using the wild-type RAF1 peptide from the 14-3-3ζ wild-type complex as template (Protein Data Bank (PDB) code 3NKX [Molzan et al., 2010]), and the -NVH residues were removed and replaced with -IH residues using the Pymol software (The PyMOL Molecular Graphics System, Version 1.5.0.4 Schrödinger, LLC). Energy minimization and computational calculations were performed according to Wodarczyk et al. [2010].

RESULTS

Exome sequencing identified 30,087 unique variants in the patient by using 8X as the coverage threshold and 25% as the allele frequency. The mean coverage was 255X, and, on average, 97.7% of the target bases were covered by at least 20 independent sequence reads. We applied sequential filters to prioritize causal mutations. In particular, we selected variants with effects on a proteins or transcripts and those that were previously unidentified or present with a MAF <1% in public datasets, including dbSNP137, the 1000 Genomes Project and ESP databases (791). We also applied inheritance models in a filtering scheme and prioritization based on the HPO. After excluding four de novo false calls due to sequencing artifacts, we detected only a de novo heterozygous three-nucleotide deletion (NM_0022880.3: c.785_787del) in the *RAF1* gene that resulted in a deletion of two amino acids and an insertion of one amino acid (p.Asn262_Val263delinsIle) (Fig. 1). This mutation was not found in the HGMD, public databases or previous publications. Because the deletion falls in the active site domain of the RAF1 binding site for the 14-3-3ζ peptide, we investigated a potential pathogenic role of Asn262_Val263delinsIle using computational modeling. We used the interfacial residues between the 14-3-3ζ protein and RAF1 peptide in the wild-type complex (PDB code 3NKX) to define a set of restraints (ambiguous interaction restraints) that were exploited in the docking calculations between the wild-type and modified RAF1 peptides and 14-3-3ζ using the HADDOCK strategy [de Vries et al., 2007]. The best HADDOCK-scored solution of the modified RAF1 peptide in complex with 14-3-3ζ is shown in Figure 2. The docked, modified RAF1 peptide interacts with the classical 14-3-3ζ binding groove and adopts an identical conformation with respect to the original RAF1 peptide in the crystallographic structure (Fig. 3) (the root mean square

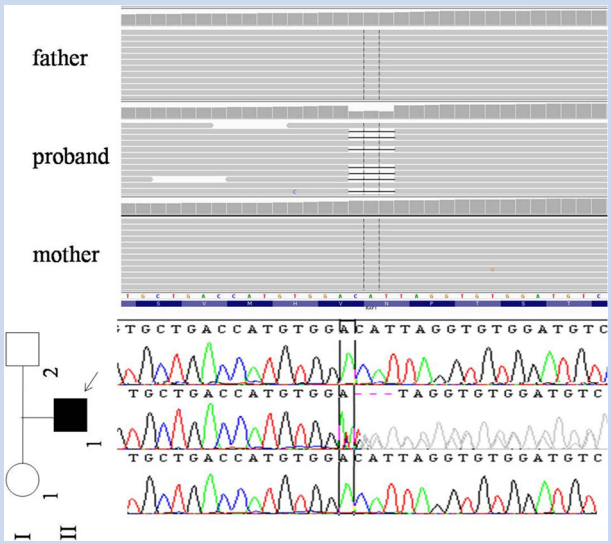

FIG. 1. Sequencing results. A: IGV browser visualization of the clinical exome sequencing results showing a de novo 3-bp deletion in the *RAF1* gene (NM_0022880.3: c.785_787del) in the patient but absent in the parents. B: Sanger sequencing confirmed the results. The reference sequence is shown at the bottom of the IGV figure. Black symbol: affected; white symbol: healthy subject at cardiac examinations.

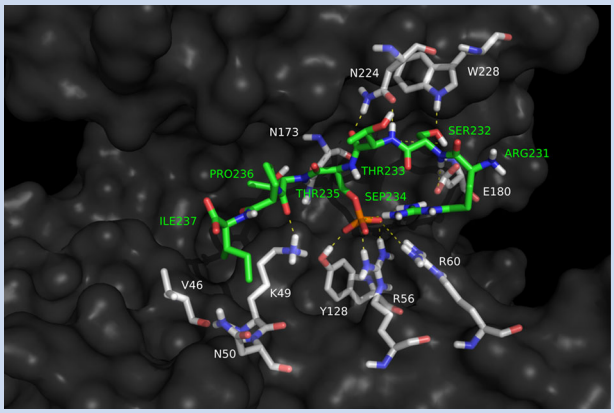

FIG. 2. HADDOCK models of the modified peptide RAF1/14-3-3ζ binding site. Surface representation of the 14-3-3ζ binding pocket in complex with the modified RAF1 peptide. The side chains of the modified RAF1 peptide that interact with the receptor are shown in green licorice, with nitrogen and oxygen atoms in blue and red, respectively. The side chains of 14-3-3ζ and the modified RAF1 that are directly involved in binding are labeled using the one- and three-letter code, respectively. SEP is the phosphorylated serine residue, and the phosphorous atom is represented in orange. Yellow dotted lines denote the hydrogen bonds of the peptide with the receptor. The model of the binding site corresponds to that with the best (lowest energy) HADDOCK score.

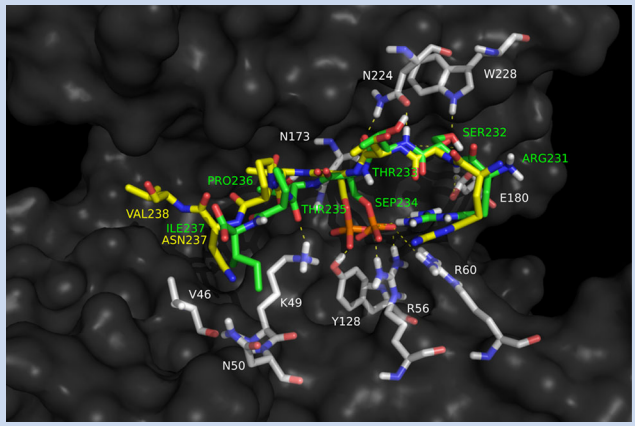

FIG. 3. Superposition of the HADDOCK structures of the modified and crystallographic RAF1 peptide in complex with 14-3-3ζ. Surface representation of the 14-3-3ζ binding pocket in complex with the modified and crystallographic RAF1 peptide. The side chains of the modified and crystallographic RAF1 peptides that interact with the receptor are shown in green and yellow licorice, respectively, with nitrogen and oxygen atoms in blue and red, respectively. The side chains of 14-3-3ζ and the modified and crystallographic RAF1 that are directly involved in binding are labeled using the one- and three-letter code, respectively. SEP is the phosphorylated serine residue, and the phosphorous atom is represented in orange. Yellow dotted lines denote hydrogen bonds of the peptide with the receptor. The shown models of the binding site correspond to those with the best (lowest energy) HADDOCK scores.

deviation (RMSD) between the backbone of the modified RAF1 with respect to the first seven residues of the original crystallographic RAF1 structure was 1.5 Å). In fact, the N-terminus of the modified RAF1 peptide performs the same interactions with the 14-3-3ζ protein, in which the SEP residue of the RAF1 peptide stably interacts with R60, R56, Y128, and K49 (Fig. 2). As expected, the difference between the modified and wild-type RAF1/14-3-3ζ complexes lies in the C-terminus. In fact, the modified RAF1 peptide cannot recapitulate the interaction with N50 of the 14-3-3ζ protein because the polar Asn residue on the original RAF1 peptide has been replaced by the apolar Ile residue in the modified RAF1 (Fig. 3). The distribution of the HADDOCK clusters is shown in Supplementary Figures S1 and S2 (see supporting information online). The binding free energies for the center of the best HADDOCK cluster were calculated using the FastContact binary [Camacho and Zhang, 2005] and Dcomplex programs [Liu et al., 2004], (the best clusters for RAF1/14-3-3ζ modified and wild-type were cluster 3 and 1, respectively). Both approaches have led to a higher affinity wild-type RAF1/14-3-3ζ complex with respect to the modified RAF1/14-3-3ζ complex ($\Delta\Delta G_{\text{modified-wild-type}} = +32$ kcal/mol and $+2$ kcal/mol using FastContact and Dcomplex, respectively). This result is in good agreement with the experimental data, where a short RAF1 peptide has a lower

affinity than a long peptide for the 14-3-3ζ protein [Molzan et al., 2010].

DISCUSSION

The differential diagnosis of these disorders, such as Noonan and LEOPARD syndrome (Noonan syndrome-multiple lentigines), is based on typical phenotypic features [Gelb and Tartaglia, 2011]. Nevertheless, these disorders are characterized by wide phenotypic variability, and clinical features are often overlapping. Moreover, the dysmorphic manifestations can be subtle and therefore overlooked; and significant changes in the clinical features occur with age [Tartaglia et al., 2011], which makes differential diagnosis and the consequent defining of therapeutic management difficult, especially in newborns. We present a two-month-old baby with biventricular hypertrophy who was referred to our hospital. Exome sequencing disclosed heterozygosity for a novel de novo 3-bp deletion in the *RAF1* gene (NM_0022880.3: c.785_787del) suggesting a diagnosis of Noonan syndrome. Biventricular hypertrophic cardiomyopathy has been previously reported in patients with Noonan syndrome features [Hirsch et al., 1975; Hayashi et al., 2001; Tozzi et al., 2013]. Known *RAF1* mutations are clustered in the conserved region domain, which carries a regulatory site for inhibition by 14-3-3 proteins proximal to the serine at position 259 [Pandit et al., 2007; Razzaque et al., 2007; Kobayashi et al., 2010]. Members of the 14-3-3 family are highly conserved proteins that are involved in signal transduction pathways, cell cycle regulation and cell survival. In particular, mutations in this site impair the phosphorylation of serine 259, resulting in partial activation of downstream extracellular signal regulated kinase (ERK) [Kobayashi et al., 2010]. Analysis of the structure of RAF1 revealed that Asn262_Val263delinsIle fell in the binding site for 14-3-3 proteins. In particular, a docking interaction study suggested that this insertion/deletion impairs binding of RAF1 to 14-3-3 proteins, resulting in constitutive activation of Ras signaling. Further studies must be performed to evaluate if p.Asn_Val263delinsIle exhibits decreased phosphorylation of serine 259.

In conclusion, we report a novel mutation that brings new insight and a deeper comprehension of the molecular basis of Noonan syndrome and could be a relevant candidate for future targeted therapies. Moreover, this approach, which combines molecular screening and in silico simulations, represents a powerful strategy to investigate the role of novel variants.

ACKNOWLEDGMENT

This work was supported by research grants from Fondazione S.Martino-CREBERG to L.P. and from Fondazione Cariplo (Ref.2011-1481) to M.E.S.

REFERENCES

Camacho CJ, Zhang C. 2005. FastContact: Rapid estimate of contact and binding free energies. Bioinformatics 21:2534–2536.

DePristo MA, Banks E, Poplin R, Garimella KV, Maguire JR, Hartl C, Philippakis AA, del Angel G, Rivas MA, Hanna M, McKenna A, Fennell TJ, Kernytsky AM, Sivachenko AY, Cibulskis K, Gabriel SB, Altshuler D, Daly MJ. 2011. A framework for variation discovery and genotyping using next-generation DNA sequencing data. Nat Genet 43:491–498.

de Vries SJ, van Dijk AD, Krzeminski M, van Dijk M, Thureau A, Hsu V, Wassenaar T, Bonvin AM. 2007. HADDOCK versus HADDOCK: New features and performance of HADDOCK2.0 on the CAPRI targets. Proteins 69:726–733.

Ewing B, Green P. 1998. Base-calling of automated sequencer traces using phred. II. Error probabilities. Genome Res 8:186–194.

Ewing B, Hillier L, Wendl MC, Green P. 1998. Base-calling of automated sequencer traces using phred. I. Accuracy assessment. Genome Res 8:175–185.

Exome Variant Server. NHLBI Exome Sequencing Project (ESP), Seattle, WA. http://snp.gs.washington.edu/EVS/. Accessed August 1, 2013.

Fantl WJ, Muslin AJ, Kikuchi A, Martin JA, MacNicol AM, Gross RW, Williams LT. 1994. Activation of Raf-1 by14-3-3 proteins. Nature 371:612–614.

Gelb BD, Tartaglia M. 2011. RAS signaling pathway mutations and hypertrophic cardiomyopathy: Getting into and out of the thick of it. J Clin Invest 121:844–847.

Hayashi S, Tojyo K, Uchikawa S, Momose T, Misawa T, Yazaki Y, Kinoshita O, Hongo M, Kubo K, Imamura H. 2001. Biventricular hypertrophic cardiomyopathy with right ventricular outflow tract obstruction associated with Noonan syndrome in an adult. Jpn Circ J 65:132–135.

Hirsch HD, Gelband H, Garcia O, Gottlieb S, Tamer DM. 1975. Rapidly progressive obstructive cardiomyopathy in infants with Noonan's syndrome. Report of two cases. Circulation 52:1161–1165.

Iascone M, Sana ME, Pezzoli L, Bianchi P, Marchetti D, Fasolini G, Sadou Y, Locatelli A, Fabiani F, Mangili G, Ferrazzi P. 2012. Extensive arterial tortuosity and severe aortic dilation in a newborn with an EFEMP2 mutation. Circulation 126:2764–2768.

Liu S, Zhang C, Zhou H, Zhou Y. 2004. A physical reference state unifies the structure-derived potential of mean force for protein folding and binding. Proteins 56:93–101.

Jain A, Chandna H, Silber EN, Clark WA, Denes P. 1999. Electrocardiographic patterns of patients with echocardiographically determined biventricular hypertrophy. J Electrocardiol 32:269–273.

Kobayashi T, Aoki Y, Niihori T, Cavé H, Verloes A, Okamoto N, Kawame H, Fujiwara I, Takada F, Ohata T, Sakazume S, Ando T, Nakagawa N, Lapunzina P, Meneses AG, Gillessen-Kaesbach G, Wieczorek D, Kurosawa K, Mizuno S, Ohashi H, David A, Philip N, Guliyeva A, Narumi Y, Kure S, Tsuchiya S, Matsubara Y. 2010. Molecular and clinical analysis of *RAF1* in Noonan syndrome and related disorders: Dephosphorylation of serine 259 as the essential mechanism for mutant activation. Hum Mutat 31:284–294.

Molzan M, Schumacher B, Ottmann C, Baljuls A, Polzien L, Weyand M, Thiel P, Rose R, Rose M, Kuhenne P, Kaiser M, Rapp UR, Kuhlmann J, Ottmann C. 2010. Impaired binding of 14-3-3 to RAF in Noonan syndrome suggests new approaches in diseases with increased Ras signaling. Mol Cell Biol 30:4698–4711.

Pandit B, Sarkozy A, Pennacchio LA, Carta C, Oishi K, Martinelli S, Pogna EA, Schackwitz W, Ustaszewska A, Landstrom A, Bos JM, Ommen SR, Esposito G, Lepri F, Faul C, Mundel P, López Siguero JP, Tenconi R, Selicorni A, Rossi C, Mazzanti L, Torrente I, Marino B, Digilio MC, Zampino G, Ackerman MJ, Dallapiccola B, Tartaglia M, Gelb BD. 2007. Gain-of-function *RAF1* mutations cause Noonan and LEOPARD syndromes with hypertrophic cardiomyopathy. Nat Genet 39:1007–1012.

Rauen KA. 2013. The RASopathies. Annu Rev Genomics Hum Genet 14:355–369.

Razzaque MA, Nishizawa T, Komoike Y, Yagi H, Furutani M, Amo R, Kamisago M, Momma K, Katayama H, Nakagawa M, Fujiwara Y,

Matsushima M, Mizuno K, Tokuyama M, Hirota H, Muneuchi J, Higashinakagawa T, Matsuoka R. 2007. Germline gain-of-function mutations in *RAF1* cause Noonan syndrome. Nat Genet 39:1013–1017.

Robinson PN, Köhler S, Bauer S, Seelow D, Horn D, Mundlos S. 2008. The human phenotype ontology: A tool for annotating and analyzing human hereditary disease. Am J Hum Genet 83:610–615.

Robinson JT, Thorvaldsdóttir H, Winckler W, Guttman M, Lander ES, Getz G, Mesirov JP. 2011. Integrative genomics viewer. Nat Biotechnol 29:24–26.

Sana ME, Iascone M, Marchetti D, Palatini J, Galasso M, Volinia S. 2011. GAMES identifies and annotates mutations in next-generation sequencing projects. Bioinformatics 27:9–13.

Schubbert S, Bollag G, Shannon K. 2007. Deregulated Ras signalling in developmental disorders: New tricks for an old dog. Curr Opinion Genet Dev 17:15–22.

Sherry ST, Ward MH, Kholodov M, Baker J, Phan L, Smigielski EM, Sirotkin K. 2001. dbSNP: The NCBI database of genetic variation. Nucleic Acids Res 29:308–311.

Stenson PD, Mort M, Ball EV, Howells K, Phillips AD, Thomas NS, Cooper DN. 2009. The Human Gene Mutation Database: 2008 update. Genome Med 1:13.

Tartaglia M, Gelb BD, Zenker M. 2011. Noonan syndrome and clinically related disorders. Best Pract Res Clin Endocrinol Metab 25:161–179.

The 1000 Genomes Project Consortium. 2012. An integrated map of genetic variation from 1,092 human genomes. Nature 491:56–65.

Thorson JA, Yu LW, Hsu AL, Shih NY, Graves PR, Tanner JW, Allen PM, Piwnica-Worms H, Shaw AS. 1998. 14-3-3 proteins are required for maintenance of Raf-1 phosphorylation and kinase activity. Mol Cell Biol 18:5229–5238.

Tidyman WE, Rauen KA. 2009. The RASopathies: Developmental syndromes of Ras/MAPK pathway dysregulation. Curr Opin Genet Dev 19:230–236.

Tozzi RJ, Abdel-Razek AM, Kipel G, Gardin JM. 2013. A unique case of a 7-year-old with noonan's syndrome, hypertrophic cardiomyopathy, biventricular outflow tract obstruction, and a right ventricular aneurysm. J Am Coll Cardiol 62:643.

Wodarczyk C, Distefano G, Rowe I, Gaetani M, Bricoli B, Muorah M, Spitaleri A, Mannella V, Ricchiuto P, Pema M, Castelli M, Casanova AE, Mollica L, Banzi M, Boca M, Antignac C, Saunier S, Musco G, Boletta A. 2010. Nephrocystin-1 forms a complex with polycystin-1 via a polyproline motif/SH3 domain interaction and regulates the apoptotic response in mammals. PLoS ONE 5:e12719.

Wu X, Simpson J, Hong JH, Kim KH, Thavarajah NK, Backx PH, Neel BG, Araki T. 2011. MEK-ERK pathway modulation ameliorates disease phenotypes in a mouse model of Noonan syndrome associated with the *RAF1* (L613V) mutation. J Clin Invest 121:1009–1025.

SUPPORTING INFORMATION

Additional supporting information may be found in the online version of this article at the publisher's web-site.